

COB-2023-0159

COMPARISON OF TEMPERATURE PROFILES AND MOLAR COMPOSITION IN THE GASIFICATION OF PETROLEUM SLUDGE.

Hiago David Zogbi Silva Oliveira

York Castillo Santiago

Universidade Federal Fluminense (UFF), Laboratório de Termociências (LATERMO), Departamento de Engenharia Mecânica (TEM/PGMEC), Universidade Federal Fluminense, Rua Passo da Pátria 156, Niterói, RJ, Brasil, CEP: 24210-240. E-mail: hiagodavid@id.uff.br, yorkcastillo@id.uff.br

Leandro Alcoforado Sphaier

Isabela Florindo Pinheiro

Universidade Federal Fluminense (UFF), Laboratório de Termociências (LATERMO), Departamento de Engenharia Mecânica (TEM/PGMEC), Universidade Federal Fluminense, Rua Passo da Pátria 156, Niterói, RJ, Brasil, CEP: 24210-240. E-mail: lasphaier@id.uff.br, isabelaflorindo@id.uff.br

Abstract. *Petroleum is composed of heavy-chain hydrocarbons, with treatment and refining processes occurring on a large scale in the petrochemical industry. Among various contaminating residues, petroleum sludge is prevalent, a highly stable emulsion of oil, water, and heavy metals, exhibiting significant energy potential. This study investigates and simulates the gasification of petroleum sludge, a thermochemical conversion process of carbonaceous materials into low- or medium-calorific value gases or intermediate agents for various gasifying agents. Hence, this article aims to comprehend the behavior of the gasification process under different conditions. Gasification cases using pure oxygen streams and atmospheric air are examined. The collected data are compared to analyze the temperature profiles along the bed and the molar fraction profiles of CH₄ and CO production in the system. For this purpose, a numerical implementation is conducted and validated using the CeSFaMB software (Comprehensive Simulation of Fluidized and Moving Bed Equipment). The temperature profiles reached 1698.7 K and 1365 K, respectively, for oxygen gasification and atmospheric air gasification cases. For the pure oxygen bed, a CO volume fraction of 28% and CH₄ volume fraction of 1.7% are achieved. Meanwhile, for the atmospheric air bed, a CO volume fraction of 12% and CH₄ volume fraction of 4% are attained. Carbon conversion to oxygen as an oxidizing agent reached approximately 97.78% for pure oxygen and 69.80% for atmospheric air. The temperature profiles fell within typical ranges for fluidized bed reactors, and the concentration profiles exhibited typical CO and CO₂ production behaviors as a function of oxygen consumption in the exothermic reactions involved.*

Keywords: *Petroleum, gasification, oil sludge, treatment, comparison*

1. INTRODUCTION

One consequence of oil's mass exploration and production is its environmental impact. The processing of oil and gas, both in the exploration sector and in the chemical industry, generates various contaminating residues that require treatment before being discarded, thus avoiding ecological imbalances from recalcitrant and toxic materials released into the environment. According to Lam *et al* (2016), atmospheric pollution due to the release of contaminants into the air, contamination of water resources, and contamination of terrestrial flora are among the numerous impacts of oil and gas exploration, production, and processing. Considering that oil and gas are essential products for the global economy and energy matrix nowadays, the importance of waste treatment methods arises to maintain biological equilibrium and social well-being.

One of the primary by-products generated during refining operations and throughout the petrochemical process is oil sludge (OS), which is the main focus of this study investigation. This residual material is produced in significant quantities. According to Gonzáles *et al* (2018), for every 500 tons of processed oil, an average generation rate of 1.0 ton (0.2 wt%) of OS. Within the context of the Brazilian petrochemical industry, refineries contribute to an annual generation of approximately 0.22 million tons of OS. Within this framework, multiple sustainable approaches exist for the disposal of OS, involving various treatments that can destabilize the emulsion or transform it into new products. These treatments encompass purely chemical, thermal or thermochemical processes. In agreement with Egazar'yants *et al* (2015), some treatment methods include landfills, incineration processes, solidification/stabilization techniques, centrifugation, and solvent extraction, among others.

These processes' limited sustainability is a significant downside, as most of their by-products lack additional value. Consequently, treatment options that yield by-products with high energy value and industrial efficiency are highly favored, as they reduce reliance on fossil resources. Thermal processes, including combustion, pyrolysis, and gasification, emerge as the most efficient methods for treating organic solids. In their research, Castillo Santiago *et al* (2021) and Jing He *et al* (2019) emphasize that this ability to generate substantial quantities of gaseous and liquid fuels containing a significant hydrocarbon content is primarily attributed to these thermal processes.

In particular, Basu (2010) outlines the gasification process as a thermochemical conversion technology, wherein carbon-rich materials like coal, biomass, or solid waste are transformed into a combustible gas referred to as producer gas. This process entails the interaction of the raw material with an oxidizing agent, which may include air, oxygen, or steam, all occurring under elevated temperature and low oxygen conditions. Also, Xu *et al* (2020) emphasized that several chemical reactions occur during gasification, including the breakdown of the feedstock's molecular structure and the formation of gases. The resulting producer gas primarily consists of carbon monoxide (CO), hydrogen (H₂), carbon dioxide (CO₂), and small amounts of other compounds such as methane (CH₄) and nitrogen (N₂). The composition and properties of the producer gas can vary depending on the feedstock used and the operational conditions of the process.

The gasification process can be conceptually divided into different stages or zones, each characterized by distinct transformations. According to Souza-Santos (2010), who suggested a framework, gasification of any solid or liquid fuel typically involves four sequential steps, referred to as zones: drying, pyrolysis, gasification, and combustion. These zones represent distinct phases of the gasification process and are associated with specific chemical and physical reactions. Gómez-Barea and Leckner (2010) have identified that temperature plays a crucial role in the transformations that occur during different stages of the gasification process. Specifically, temperature-dependent transformations are observed in the drying stage, primary pyrolysis stage, and a portion of the secondary pyrolysis stage. On the other hand, chemical transformations primarily occur in the gasification, partial combustion, and another amount of the secondary pyrolysis stage. These chemical reactions can occur between gases, known as homogeneous reactions, or between a gas and a solid, known as heterogeneous reactions. A comprehensive understanding of the gasification process can be obtained by distinguishing between temperature-driven transformations and chemical reactions. Gasifiers can be classified based on the behavior of the bed, which can be fixed, fluidized, or entrained. According to Speight (2013), gasifiers are classified as follows: Fixed bed gasifiers, which are further subdivided into countercurrent and concurrent flow; fluidized bed gasifiers, which consist of two types, bubbling and circulating fluidized beds; and entrained flow gasifiers, in which the bed ceases to exist, and the solids are introduced in a pneumatic conveying process.

Due to the complexity and importance of the gasification process, as well as the use of oil residues, several studies have been conducted to understand and optimize the process. For example, Ashizawa *et al* (2005) studied the gas temperature profile and heat flow distribution in a research-scale entrained-flow gasifier using oxygen as the oxidant. The results showed a variation in the average bed temperature range according to the Oxygen/Carbon (O/C) ratio, indicating a tendency for higher temperatures with increasing oxygen in the system. The average bed temperature at $Z = 1000$ mm yielded results of 1290°C for 0.37 O/C and 1430°C for 0.4 O/C. Significant heat flux was observed in the range of $Z = 1000$ -1500 mm, with values ranging from 3000 to 5000 W/m², primarily at the top of the reactor, indicating a region of intense reaction rate between fuel and oxygen, resulting in high temperatures in that area.

Tremel *et al* (2012) examined the analysis of coal gasification using entrained flow. The oxygen was consumed instantaneously after the coal feed was started and entered the reaction zone. The concentrations of the gasification products, CO, H₂, and CO₂, increased. The gas concentrations stabilized at nearly constant values during the test. The CO concentration increased from 6% to 7% in a residence time of 1.4 s and reached 12% in 3.0 s, while CO₂ is consumed, and its concentration decreased from 6% to 2.5%. The result for a residence time of 1.0 s was a conversion of 94% at 0.5 MPa in the first reactor at 1200 °C, an increase to 1600 °C at 0.5 Mpa, and an increase in residence time of 1.3 s, resulting in a coal conversion of 97%. The authors concluded that the conversion increases with temperature and residence time. The increase is more significant from 1200 °C to 1400 °C compared to 1400 °C to 1600 °C, indicating a progressive influence of mass transfer limitations.

Bader *et al* (2018) conducted a heavy oil gasification experiment. The pressure was set at 60 bar, with 446 kg/h of heavy oil driven by 101 kg/h of steam into the reactor. 455 kg/h of oxygen and 78 kg/h of steam were injected. The heavy oil's net calorific value is measured internally at 40 MJ/kg. The oil is converted to producer gas and soot. The dry gas composition at the outlet is determined in various heavy oil and natural gas gasification tests. The outlet temperature was 1599 K. The conversion reached ranges of 97.92 - 98.78%.

In this study, the concept of gasification and data from previous research were applied to examine the behavior of the process using various oxidizing agents (pure oxygen and atmospheric air). The objective was to observe how temperature and mole fraction profiles change as a function of space. The temperature and mole concentration profiles were acquired via CeSFaMB (Comprehensive Simulation of Fluidized and Moving Bed Equipment) software for entrained bed gasifiers. These profiles were analyzed to comprehend the behavior of entrained bed gasifiers, serving as an example for evaluating economic feasibility and opportunities for cost reduction and production maximization.

2. MATERIALS AND METHODS

The present work aims to analyze quantitatively the behavior of producer gas's temperature bed and molar concentration profiles. A mathematical model developed by Souza-Santos (2010) is implemented. This model is constructed to calculate mass and energy balances in various equipment used in the chemical industry, including gasifiers. Due to the complexity of the gasification process, the model incorporates several simplifications that allow for numerical convergence and the acquisition of data close to reality. The main simplified assumptions are as follows:

- One-dimensional model;
- The system operates under steady-state conditions;
- The bed model consists of two phases;
- The circulation rate always produces a homogeneous composition of solid particles in the bed;
- There is no axial heat transfer;
- A plug-flow regime is adopted, assuming the gas in the chamber has no rotational movement;
- Heat dissipation due to viscosity and diffusive effects is neglected;
- The reaction occurs over a sufficient time, assuming that the fuel gas is completely diluted at the injection point.

Simulations based on these assumptions of the Souza-Santos (2010) model are performed using a commercial software called CeSFaMBTM (Comprehensive Simulation of Fluidized and Moving Bed Equipment), also known as CSFMB. The software operates based on input data (inputs), and among the variety of inputs, the main ones are convergence parameters, geometric data, oxidant flow data, and fuel flow data.

The present research utilizes experimental data imported from the literature (Ashizawa *et al*, 2005). As previously mentioned, the authors worked with an extra-heavy oil known as Orimulsion®, which is a liquid fossil fuel produced from a mixture of crude oil and water (its composition is presented in Table 1), with the addition of emulsifiers.

Table 1: Orimulsion® elemental analysis.

Immediate Analysis Wet Base	Mass Percentage	Ultimate analysis Dry base	Mass Percentage	Higher heating value [MJ/kg]
Moisture	28.80%	C	84.28%	29.76
Ash	0.18%	H	10.33%	-
Fixed carbon	12.84%	O	0.55%	-
Total sulfur	2.81%	N	0.64%	-
Volatile	55.37%	S	3.95%	-
-	-	Ash	0.25%	-

3. MODELING DATA INPUT

3.1. Reactor Geometry

As mentioned above, this work imports data from the literature into the process simulation. The same applies to the reactor structure, where data is imported from the experimental research by Ashizawa *et al* (2005). The gasifier used by Ashizawa is an industrial-scale model with a capacity to process 2.4 tons/day and was designed by the Central Research Institute of Electric Power Industry (CRIEPI) in Yokosuka, Japan, to investigate various phenomena occurring in the gasifier, including chemical reactions and gasifier performance indicators. It has a height of 3000 mm, and the diameter of the cylindrical internal section has a value of 300 mm. It is operated in a downdraft geometry, meaning that the inlet flow is introduced from the top, adopted as the $Z = 0$ point (vertical axis).

3.2 Main reactions considered.

The gasification process is a complex thermochemical process with several chemical reactions. The CeSFaMB model considers many reactions, significantly representing the process's reality. Table 2 below shows the main reactions that are considered in the oil sludge gasification process studied.

Table 2. Chemical reactions for OS gasification process.

Reaction Number	Chemical Reaction	Heat of reaction (kJ/mol)	Reaction name
R1	Oil sludge → volatiles + char	0	Oil sludge pyrolysis
R2	$H_2 + 1/2O_2 \rightarrow H_2O$	-242	H ₂ oxidation
R3	$CO + 1/2O_2 \rightarrow CO_2$	-238	CO oxidation
R4	$C + 1/2O_2 \rightarrow CO$	-111	Char partial oxidation
R5	$C + O_2 \rightarrow CO_2$	-394	Char total oxidation
R6	$CO + H_2O \rightleftharpoons CO_2 + H_2$	-41	Water-gas shift reaction
R7	$C + CO_2 \rightleftharpoons 2CO$	+172	Boudouard Reaction
R8	$C + H_2O \rightleftharpoons CO + H_2$	+131	Char gasification
R9	$C + 2H_2 \rightleftharpoons CH_4$	-75	Char hydrogenation
R10	$CH_4 + H_2O \rightleftharpoons CO + 3H_2$	+206	Steam methane reforming

3.3. Convergence parameter adopted

The initial conversion values, factors that help convergence, and the criteria that establish the convergence behavior are defined for simulation. The convergence parameter inputs required to simulate the process in CeSFaMB are shown in Table 2.

Table 2: Convergence parameter adopted

Minimum carbon conversion (CCMINP)	70%
Maximum carbon conversion (CCMAX)	90%
Convergence criteria	1.D-06

Among the conversion criteria, CCMINP and CCMAX act as a starting point for the convergence path, limiting it to the best possible conversion to obtain high carbon conversion efficiencies.

3.4. Input parameters for oxidizing agent and fuel

Two distinct scenarios were considered to investigate the temperature and molar composition profiles. Each scenario used different gasification agents, specifically pure oxygen and atmospheric air. In this study, the Equivalence Ratio (ER) concept will be employed when considering air and oxygen as gasification agents. Consequently, ER is defined as the ratio between the amount of fuel and the amount of the gasifying medium under actual operational conditions, divided by the same ratio under stoichiometric conditions, as presented in Eq (1).

$$ER = \frac{(\dot{Q}_{O_2}/\dot{Q}_{OS})}{(\dot{q}_{O_2}/\dot{q}_{OS})_{st}} \quad (1)$$

Where \dot{Q}_{O_2} and \dot{Q}_{OS} are the mass flows of OS and oxygen, respectively. In addition, \dot{q}_{O_2} and \dot{q}_{OS} represent the stoichiometric (st) mass flows of OS and oxygen, which is the required flow for complete oxidation. Table 3 shows the airflow results for the chosen equivalence ratio based on Eq (1).

Table 3: Airflow for Equivalence Ratio variation, using 100 kg/h of Orimulsion.

Equivalence Ratio	Air (Kg/h)	Rate Air/C
0.2	265.6	2.656
0.25	332	3.32

Table 4 shows the input values used for the simulation. As the aim was only to evaluate the typical behavior of a temperature and molar concentration profile, there was no significant variation in the input parameters apart from the type of oxidant.

Table 4: Oxidizing agent input data

Oxidant	Atmospheric Air	Oxygen
Flow (kg/h)	265.6	75.6
Temperature (K)	1500 - 2000	1500 - 2000
Pressure (kPa)	1900	1900

3.5. Validation Model

Experimental work is limited in the literature on this line of research. To validate the simulation, we used the experimental data from Ashizawa *et al* (2005) for an entrained flow reactor with oxygen at 0.4 ER. As already mentioned, the fuel used was Orimulsion, a heavy oil that is very similar in experimental terms to OS. The deviation between the model results and the experimental data was quantified using the root mean square error (RMS), given by Eq (2).

$$RMS = \sqrt{\frac{\sum_i (exp_i - mod_i)^2}{N}} \quad (2)$$

In this case, exp_i are the experimental data obtained in the literature, mod_i are the values from the developed model, and N indicates the total number of measures.

Figure 1 shows the difference between the gasification gas volume fractions obtained from the experimental tests of Ashizawa *et al* (2005) and those of the present work. This comparison was made using the root mean square error (RMS), and it is possible to see agreement below 5%, which proves acceptable. Based on Eq (2) and Figure 1, the RMS was obtained, reaching approximately 1.6% for the data simulated in this work.

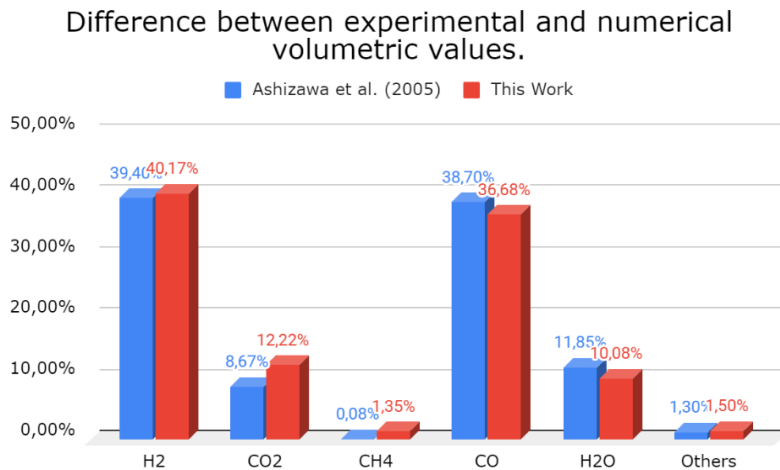


Figure 1. Difference between experimental and numerical volumetric values.

4. RESULTS AND DISCUSSION

4.1 Comparison of temperature profiles

Since the initial focus was not to study the influence of the equivalence ratio (ER), values between 0.2 and 0.25 were used, which best fit the desired temperature profiles. The average temperature variation for this range of ER is tiny, so it was not considered. The process simulation resulted in the temperature profiles shown in Figures 2 and 3.

For the process shown in Figure 2, carbon conversion reached a range of 69.8%. The average temperature of the bed was around 1365 K, and the residence time of the particles in the bed was 18.77 s. Analyzing the profile, a significant increase in temperature can be seen at $Z = 1$ m, which can be concluded as a range where exothermic reactions, such as partial and total oxidation of char (R4 and R5) and oxidation of hydrogen and carbon monoxide (R2 and R3) occurred mainly. From this point on, the temperature undergoes few variations in space, following a value close to convergence in the bed. In the process considered, the pyrolysis and drying stages (R1) occur instantaneously at $z = 0$ m.

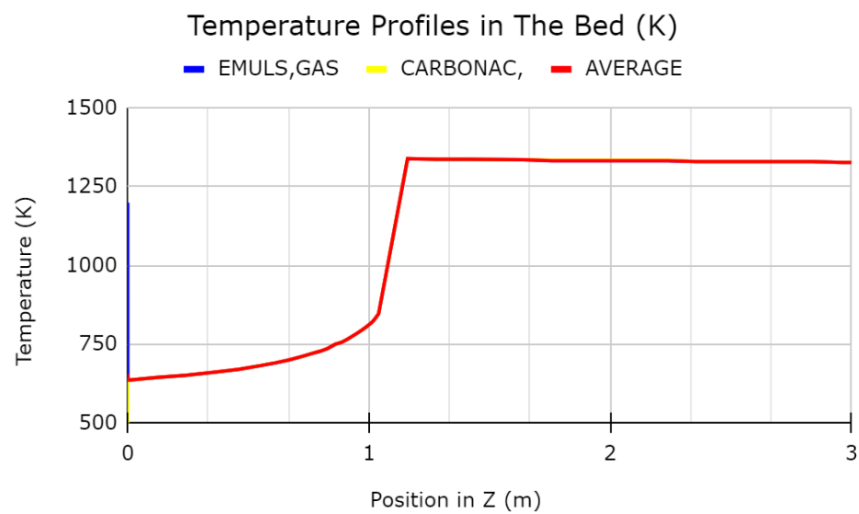


Figure 2: Temperature profile for air carrier bed.

The carbon conversion for the process observed in Figure 3 was 95.78%. The temperature in the bed reached a maximum of 1923 K, while the average temperature was maintained at 1698.7 K, with an observed residence time of 6.8 s. Temperature increases and exothermic reactions occur at $Z = 0.08$ m, reaching a range of 1947 K at the start of the bed and remaining constant in the 1600 K range. The drying and pyrolysis process also occurred instantaneously at $Z = 0$ m.

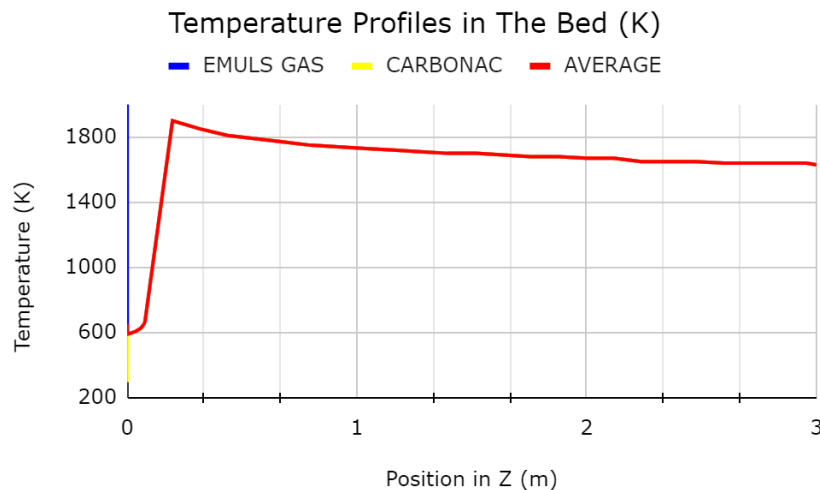


Figure 3: Temperature profile for oxygen carrier bed.

The bed temperature increased and remained higher when O₂ was used as the gasification agent compared to atmospheric air, as deduced by studying the comparison of temperature profiles in Figure 4. For pure oxygen, oxidation reactions (R2 to R5) occur more frequently compared to a mixture of O₂ and N₂ (found in atmospheric air), where the high nitrogen concentration limits the reaction rate due to its inert nature. Nitrogen dilutes the production gas and does not contribute energetically to the reactions, reducing the temperature profile (Castillo Santiago *et al*, 2021). The residence time of particles in the bed shows similar results in value of 6.77s, with exothermic reactions occurring faster in the oxygen profile compared to the air profile.

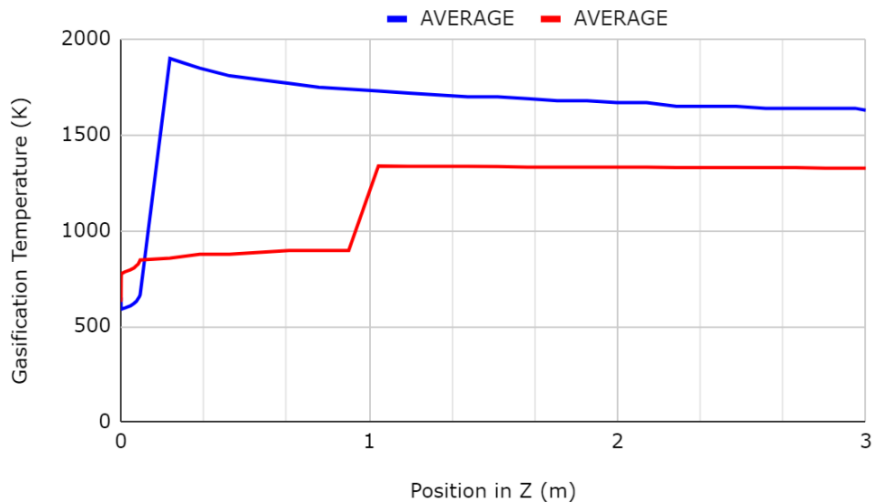


Figure 4: Comparison of Temperature profile.

4.2 Comparison of molar profiles.

For the gasification process with air as a gasifying agent, Figure 5 shows a similar increasing behavior for the molar fractions as a function of oxygen consumption in the bed. The CO curve for both cases grows faster because of the incomplete oxidation of the carbonaceous material. As mentioned in the temperature profiles, at the Z = 1 m point, the increase in temperature indicates the range where the exothermic reactions occurred with greater intensity, and through the mole fraction profile, it is possible to observe the rise in the concentration of the reaction products (R2 to R5).

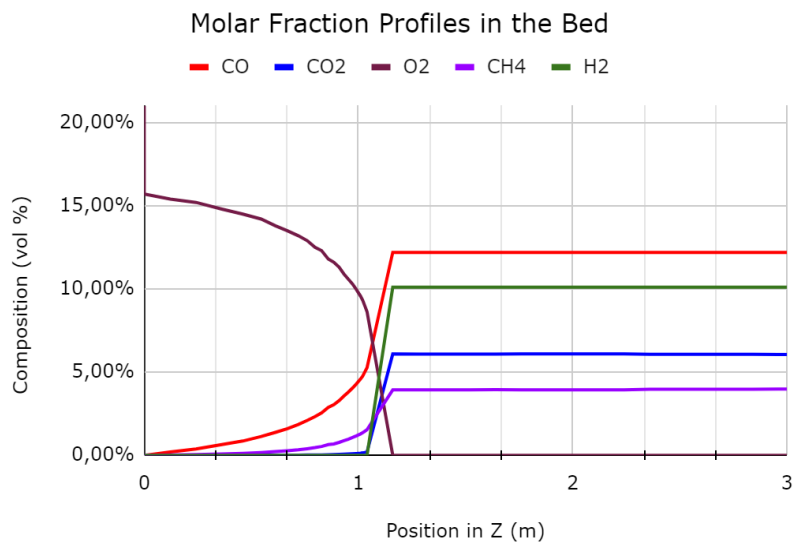


Figure 5: Molar concentration profile for air gasification. (O₂, CO₂, CO, CH₄ and H₂)

Figure 6 shows the molar profiles of O₂, CO₂, CO, H₂O, CH₄, and H₂ for gasification with oxygen. For this case, it was observed that the oxidation reactions intensified from Z =0.4 m, producing CO₂ and CO in the system and depleting the available O₂.

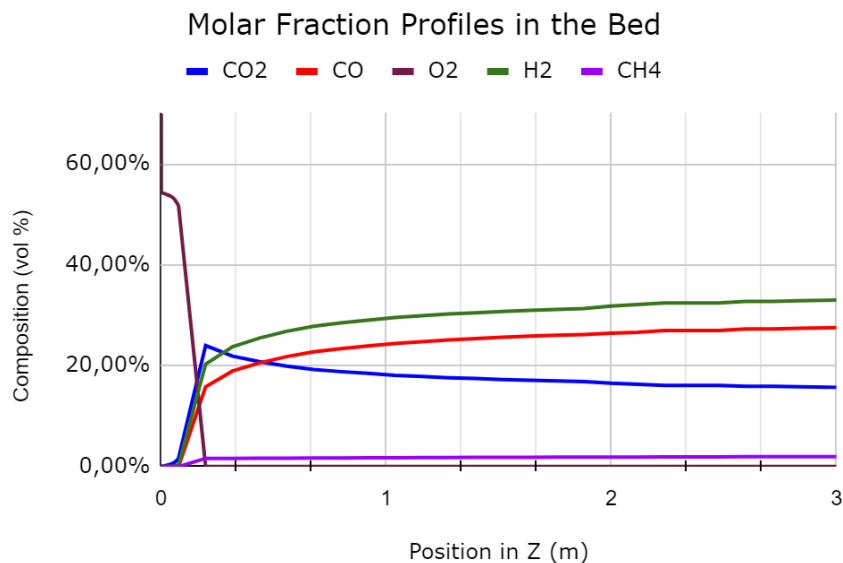


Figure 6: Molar concentration profile for oxygen gasification (O₂, CO₂, CO, CH₄ and, H₂)

The comparative graph of the CO concentration profile in OS gasification for oxygen and atmospheric air (Figure 7) shows values of about 28% and 12%, respectively, indicating a higher CO production for oxygen as the gasifying agent. This is because at higher temperatures, endothermic reactions such as the Boudouard reaction (R7) are favored by shifting the chemical equilibrium according to the le Chatelier principle (Castillo Santiago *et al*, 2021).

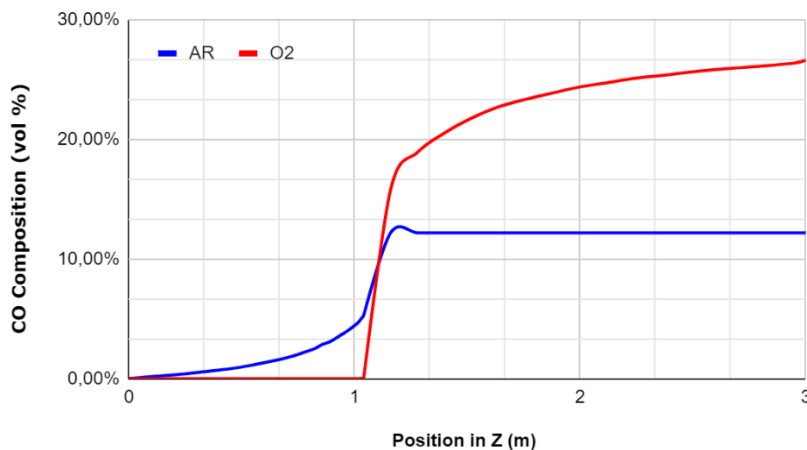


Figure 7. CO composition profile for atmospheric air bed and pure oxygen bed

However, in Figure 8, the methane concentration profile showed the opposite characteristic, where values of approximately 4% and 1.7% methane were obtained for atmospheric air and oxygen, respectively. This indicates a greater presence of the char hydrogenation reaction (R9) for the bed with atmospheric air and a higher presence of the methane steam reforming reaction (R10) for the bed with pure oxygen.

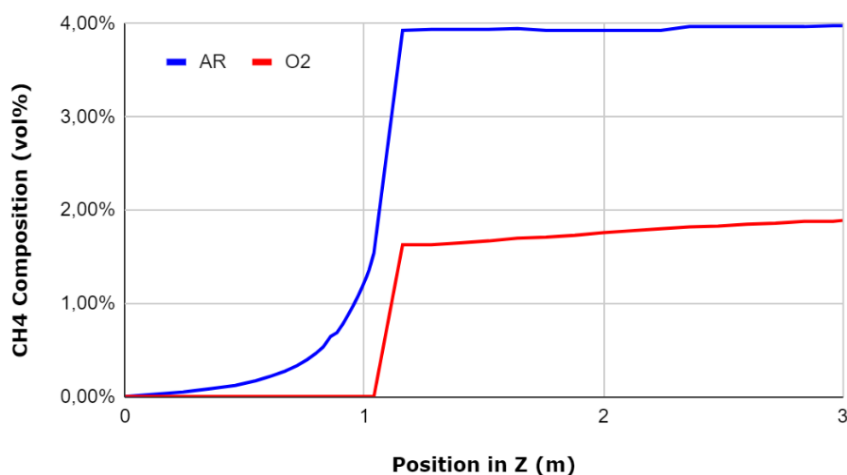


Figure 8. CH₄ composition profile for atmospheric air bed and pure oxygen bed

5. CONCLUSION

Based on the results obtained and the conducted analyses, it can be concluded that gasification simulation using pure oxygen as the oxidizing agent exhibited superior performance in carbon conversion and CO production compared to atmospheric air. Pure oxygen use resulted in lower CH₄ production than atmospheric air, which may be an essential factor in selecting the oxidizing agent for gasification systems, depending on specific production interests and requirements. Furthermore, it was observed that the average bed temperature significantly impacted carbon conversion, but oxygen availability had an even more influential effect on this process. The oxygen concentration decreased sharply in the system fueled with pure oxygen, indicating higher oxygen consumption and more substantial production of CO and CO₂. Considering the economic aspects, the results obtained can impact the efficiency and cost of the process in an industrial plant. Maximizing the production of the desired product, such as H₂ and CO, can lead to better use of resources and optimization of operating costs. It is important to note that the choice of oxidizing agent must consider a comprehensive analysis of the process conditions and the specific objectives of the application. Therefore, further studies and economic analysis are needed to fully evaluate the potential application of these results on an industrial scale.

6. ACKNOWLEDGEMENTS

We want to thank FAPERJ immensely for the support provided (Grants n° 204.503/2022 and 200.261/2023). We would also like to thank Professor Dr. Marcio L. de Souza-Santos, for providing the software that allowed this work. Finally, we would like to thank the Universidade Federal Fluminense for making LATERMO (Thermal Sciences Laboratory of UFF) available for studies in thermodynamics and the National Agency of Petroleum, Natural Gas and Biofuels (PRH-ANP No 51.1).

7. REFERENCES

- Ashizawa, M., Hara, S., Kidoguchi, K., & Inumaru, J. (2005). Gasification characteristics of extra-heavy oil in a research-scale gasifier. *Energy*, 30(11-12 SPEC. ISS.), 2194–2205. <https://doi.org/10.1016/j.energy.2004.08.023>.
- Bader, A., Hartwich, M., Richter, A., & Meyer, B. (2018). Numerical and experimental study of heavy oil gasification in an entrained-flow reactor and the impact of the burner concept. *Fuel Processing Technology*, 169, 58–70. <https://doi.org/10.1016/j.fuproc.2017.09.003>.
- Basu, P. (2008). *Biomass Gasification, Pyrolysis and Torrefaction - Practical Design and Theory* (Vol. 2).
- Castillo Santiago, Y., Martínez González, A., Venturini, O. J., & Yepes Maya, D. M. (2021). Assessment of the energy recovery potential of oil sludge through gasification aiming electricity generation. *Energy*, 215. <https://doi.org/10.1016/j.energy.2020.119210>.
- Egazar'yants, S. V et al. Oil Sludge Treatment Processes. *Chemistry and Technology of Fuels and Oils*, v. 51, n. 5, p. 506–515, 2015. Available at: <<https://doi.org/10.1007/s10553-015-0632-7>>.
- Gómez-Barea, A., & Leckner, B. (2010). Modeling of biomass gasification in fluidized bed. In *Progress in Energy and Combustion Science* (Vol. 36, Issue 4, pp. 444–509). Elsevier Ltd. <https://doi.org/10.1016/j.pecc.2009.12.002>;
- He, J., Strezov, V., Kumar, R., Weldekidan, H., Jahan, S., Dastjerdi, B. H., Zhou, X., & Kan, T. (2019). Pyrolysis of heavy metal contaminated *Avicennia marina* biomass from phytoremediation: Characterisation of biomass and

- pyrolysis products. *Journal of Cleaner Production*, 234, 1235–1245. <https://doi.org/10.1016/j.jclepro.2019.06.285>
- James G Speight. (2013). *Heavy and Extra-heavy Oil Upgrading Technologies* (1st ed., Vol. 1).
- Lam, S. S., Liew, R. K., Jusoh, A., Chong, C. T., Ani, F. N., & Chase, H. A. (2016). Progress in waste oil to sustainable energy, with emphasis on pyrolysis techniques. In *Renewable and Sustainable Energy Reviews* (Vol. 53, pp. 741–753). Elsevier Ltd. <https://doi.org/10.1016/j.rser.2015.09.005>.
- Martínez González, A. et al. Hydrogen production from oil sludge gasification/biomass mixtures and potential use in hydrotreatment processes. *International Journal of Hydrogen Energy*, v. 43, n. 16, p. 7808–7822, 2018.
- Souza-Santos, M. L. de. (2010). *Solid fuels combustion and gasification : modeling, simulation, and equipment operations*. Taylor & Francis.
- Speight, J. G. (2015). Types of gasifier for synthetic liquid fuel production: Design and technology. In *Gasification for Synthetic Fuel Production: Fundamentals, Processes and Applications* (pp. 29–55). Elsevier Ltd. <https://doi.org/10.1016/B978-0-85709-802-3.00002-3>.
- Tremel, A., Haselsteiner, T., Kunze, C., & Spliethoff, H. (2012). Experimental investigation of high temperature and high pressure coal gasification. *Applied Energy*, 92, 279–285. <https://doi.org/10.1016/j.apenergy.2011.11.009>.
- Turns, S.R. An introduction to combustion. Concepts and applications. Ed. McGraw-Hill. 2000.
- Xu, D., Xiong, Y., Ye, J., Su, Y., Dong, Q., & Zhang, S. (2020). Performances of syngas production and deposited coke regulation during co-gasification of biomass and plastic wastes over Ni/γ-Al₂O₃ catalyst: Role of biomass to plastic ratio in feedstock. *Chemical Engineering Journal*, 392. <https://doi.org/10.1016/j.cej.2019.123728>.

8. RESPONSIBILITY NOTICE

The authors are the only responsible for the printed material included in this paper.